Quantitative *In situ* Analysis of β-Catenin Expression in Breast Cancer Shows Decreased Expression Is Associated with Poor Outcome

Marisa Dolled-Filhart, Anthony McCabe, Jennifer Giltnane, Melissa Cregger, Robert L. Camp, and David L. Rimm

Department of Pathology, Yale University School of Medicine, New Haven, Connecticut

Abstract

The role of β-catenin in breast cancer and its prognostic value is controversial. The prognostic value had been assessed previously in a series of nonquantitative immunohistochemical studies with conflicting results. In efforts to clarify the relationship between β-catenin protein expression and breast cancer prognosis, we have assessed a retrospective 600 case cohort of breast cancer tumors from the Yale Pathology archives on tissue microarrays. They were assessed using automated quantitative analysis (AQUA) with a series of array-embedded cell lines for which the β-catenin concentration was standardized by an ELISA assay. The expression levels of the standard clinical markers HER2, estrogen receptor (ER), progesterone receptor (PR), and Ki-67 were also assessed on the same cohort. X-tile software was used to select optimal protein concentration cutpoints and to evaluate the outcome using a training set and a validation set. We found that low-level expression of membranous β-catenin is associated with significantly worse outcome (38% versus 76%, 10-year survival, validation set log-rank $P = 0.0016$). Multivariate analysis of this marker, assessed in a proportional hazards model with tumor size, age, node status, nuclear grade, ER, PR, HER2, and Ki-67, is still highly significant with a hazard ratio of 6.8 ($P < 0.0001$, 95% confidence interval, 3.1-15.1). These results suggest that loss of β-catenin expression at the membrane, as assessed by objective quantitative analysis methods, may be useful as a prognostic marker or may be part of a useful algorithm for prognosis in breast cancer. (Cancer Res 2006; 66(10): 5487-94)

Introduction

β-Catenin is a critical component of cadherin-based cell-cell adhesion and also a regulatory node of the *wnt* signaling pathway. It links cadherins indirectly to the actin cytoskeleton and is subject to tyrosine phosphorylation as a mechanism to regulate adhesion. It also interacts with members of the LEF/TCF family of transcriptional activators as a critical intermediate in signal transduction pathways. Serine and threonine phosphorylation regulate its stability, targeting it to degradation through an APC-mediated proteosomal pathway or to the nucleus to activate transcription of a number of proteins associated with cellular transformation (1). Thus, *β-catenin* is considered an oncogene and its dysregulation or mutational activation can lead to cancer (2). Unlike colorectal carcinoma, hepatocellular carcinoma, or some other less common tumors that have a high frequency of β-catenin mutations, mutations are very rare in breast cancer (3). However, there are multiple lines of evidence that suggest β-catenin plays a role in breast cancer (reviewed in refs. 4, 5). Thus, it is likely that its role in breast cancer is a function of its level of expression or activation.

Previous immunohistochemical analyses of β-catenin in breast cancer tumors have shown mixed results regarding localization and relationship with patient outcome. Dillon et al. (6) showed no relationship between β-catenin expression and outcome in a cohort of 91 patients. Nakopoulou et al. (7) examined 51 invasive ductal carcinomas by semiquantitative immunohistochemical analysis and found that membranous expression was significantly associated with low histologic grade tumors ($P = 0.04$) and positive estrogen receptor (ER) expression ($P = 0.045$). Abnormal (reduced) β-catenin expression was significantly associated with a high rate of infiltrating lymph nodes ($P = 0.016$), advanced stage of disease ($P = 0.02$), and presence of lymph node metastases ($P = 0.016$). An examination of 121 breast cancer tumors by Karayiannakis et al. (8) showed retention of normal membranous β-catenin staining in 32% of invasive ductal carcinomas but did not report correlation with outcome. In an examination of 90 primary breast cancers by Bukholm et al. (9), 55.6% of tumors had reduced or absent membranous staining but there was no relationship with expression and metastasis. Semiquantitative immunohistochemical analysis of 55 invasive ductal breast tumors by Bankfalvi et al. (10) showed that 36% had reduced membranous β-catenin expression, all of which were in less differentiated tumors (grades 2 and 3). The reduced β-catenin expression correlated with positive lymph node status ($P = 0.03$) but there was no significant relationship between β-catenin expression and patient survival. Thus, the overall conclusion of this series of studies was that decreased β-catenin staining was associated with poor prognostic factors.

Then, in complete contradiction to previous studies, an analysis of 123 primary breast cancer tumors by Lin et al. (11) of Mien-Chie Hung's group showed that high β-catenin expression in nuclei was associated with poorer prognosis in patients compared with tumors with membranous β-catenin expression ($P < 0.0001$) and that it was an independent predictive marker in multivariate analysis ($P = 0.001$). Although nuclear staining has been reported in many tumor types, especially colon (12, 13), this group was the first and only group to find it in breast cancer with prognostic value, although another paper assessing 40 breast cancer samples designated 62.5% as cytoplasmic/nuclear β-catenin positive (14). Several additional articles report a lack of nuclear β-catenin

Note: M. Dolled-Filhart and A. McCabe contributed equally to this work.
Requests for reprints: David L. Rimm, Department of Pathology, Yale University School of Medicine, 310 Cedar Street, PO Box 208023, New Haven, CT 06520-8023. Phone: 203-737-4204; Fax: 203-737-5089; E-mail: david.rimm@yale.edu.

doi:10.1158/0008-5472.CAN-06-0100

staining. Pedersen et al. (15) reported no relationship to patient survival in 61 breast cancer tumors by the same method as the Hung group. A similar immunohistochemical breast cancer tumor study looking at protein expression correlations between *wnt* signaling pathway components by Wong et al. (16) also did not see any β-catenin nuclear staining. The largest cohort to date to assess β-catenin expression in breast cancer was that of Gillet et al. (17). They found no significant difference in patient outcome between low (22%) and high (88%) membranous staining, with negligible nuclear β-catenin staining in 470 patients. Thus, there is one report of nuclear expression of β-catenin with a compelling association with outcome. These conflicting observations led us to reexamine β-catenin expression in a large cohort of breast cancer tumors using more quantitative methods.

Tissue microarrays (18–20) are an efficient way to evaluate hundreds of tumors without extensive damage to the original tumor sample. Additional benefits to this method are that all samples are treated under identical antigen retrieval and staining conditions. Use of a grid format allows for each tumor to be linked to its respective clinical and pathologic information in a database. Several studies have shown that a single breast cancer tissue microarray core is sufficient to represent the expression seen on whole sections on a population level with clinical end points (21–23).

A set of algorithms called automated quantitative analysis (AQUA) has been developed in our laboratory that allows for rapid analysis of immunofluorescence on tissue microarrays (12). Automated analysis reduces the amount of human variability in scoring immunohistochemical staining by eye and results in a continuous range of protein expression AQUA scores of rather than ordinal (0, +1, +2, and +3) scores. AQUA allows for quantification of the marker (protein of interest) within user-defined subcellular compartments within the tumor region of each tissue microarray spot. Figure 1 shows an illustration of how AQUA works with an example of ER staining on a breast cancer tissue microarray core.

An often used method to assess the difference between the high- and low-expression groups of a population is by division of populations into quartiles, quintiles, or deciles. Often, immunostaining studies use the ordinal scores of 0, +1, +2, and +3 to show such divisions. However, these arbitrary divisions may not accurately reflect the biology of biomarker expression and may be limited by the capability to accurately sense subtle differences in staining colors when scored by eye. This study uses a new method of parsing expression data and choosing expression level cutpoints called X-tile, which was recently developed in our laboratory (24).

Materials and Methods

Cell line culture. NCI-H28, SK-BR-3, MCF-7, MDA-MB-435, T-47-D, BT-474, A-431, and SW-480 were used in this study. The cell lines T-47D, MDA-MB-435, SK-BR-3, and SW-480 were purchased from American Type Culture Collection (Manassas, VA). SK-BR-3, A-431, and SW-480 were cultured in DMEM with 10% fetal bovine serum (FBS) and 1% penicillin/streptomycin. T-47D, MCF-7, BT-474, MDA-MB-435, and NCI-H28 were routinely maintained in RPMI 1640 supplemented with 10% FBS and 1% penicillin/streptomycin. All cell lines were maintained in a 37°C incubator with 5% CO_2.

β-Catenin detection by ELISA. β-Catenin protein was detected in the cell lines by ELISA using the DuoSet IC Human Total β-catenin ELISA (R&D Systems, Minneapolis, MN). Ten-centimeter plates of the cell lines were washed in cold 1× PBS and then incubated for 30 minutes at 4°C in radioimmunoprecipitation assay buffer supplemented with a protease inhibitor cocktail, which included Pefabloc and CLAP (chymostatin, leupeptin, antipain, and pepstatin A). Total protein was measured using the BCA protein detection method (Pierce). Cell lysates were aliquoted and stored at −80°C. Cell lysates were diluted to 0.1 mg/mL in lysis buffer for use in the β-catenin ELISA. The ELISA was done as per the instructions of the manufacturer; all standards and samples were done in duplicate. β-Catenin concentrations in the cell lysates were determined from the resultant standard curve and are expressed as ng/mg protein lysate.

Tissue microarray construction and cohort details. Tissue microarrays were constructed from archival formalin-fixed, paraffin-embedded breast cancer specimens as previously described and reviewed (25, 26). Briefly, representative regions were selected for coring by pathologists based on the corresponding H&E-stained full sections. The tissue microarray was constructed with single 0.6-mm-diameter cores of each case spaced 0.8 mm apart in a grid format using a Tissue Microarrayer (Beecher Instruments, Sun Prairie, WI). The tissue microarray block was then cut into 5 μm sections with a microtome, adhered to the slide by an adhesive tape-transfer method (Instrumedics, Inc., Hackensack, NJ) and UV cross-linked. The breast cancer cohort consists of 688 samples of invasive ductal carcinoma selected from the Yale University Department of Pathology archives as available from 1961 to 1983. The mean follow-up time of this cohort is 12.8 years and the mean age of diagnosis is 58.1 years. The median follow-up time is 8.9 years and the median age of diagnosis is 58.0 years. Of the 656 patients with follow-up time, 328 were censored at 20 years and 276 were uncensored at 20 years. Of the 328 censored patients, their median follow-up was 21.4 years, with the minimum at 4.2 months. This cohort contains approximately half node-positive specimens and half node-negative specimens, which have been used previously in other studies from our laboratory (27–32). Complete clinical treatment information was not available for this cohort; however, some limited information was available for the node-positive patients. Most node-negative patients were treated with local radiation, and none received Herceptin. About 15% of the node-positive patients were treated with chemotherapy (primarily Adriamycin, cytoxan, and 5-fluorouracil), and subsequently ~27% received tamoxifen (post-1978). The node-negative patients were largely treated only by surgical resection.

Cell line microarray construction. The cell lines were cultured on 75 cm^2 tissue culture flasks as described above. Once the cells reached 90% confluence, the cells were washed twice in 1× PBS and 5 mL neutral buffered formalin were added to the cells for 5 minutes at room temperature. After 5 minutes, the cells were removed from the flask with a cell scraper. The cells were stored at 4°C in the neutral buffered formalin. To make a cell line microarray, a donor block of each of the cell lines was first made; this was done as follows: the cells collected in neutral buffered formalin were centrifuged at room temperature at 1,500 rpm for 10 minutes. The supernatant was removed and the cells were resuspended in 500 μL of 80% ethanol. The cells were then centrifuged at 12,000 rpm for 5 minutes after which the supernatant was removed. The resultant pellet was mixed with 50 to 150 μL warm (55°C) 1% low melt agarose (made in 1× PBS) and the cell slurry was transferred to the cap of a 1.5 mL Eppendorf tube and allowed to solidify at room temperature; this step is done as quickly as possible to avoid the agarose solidifying before being added to the Eppendorf cap. Once the cell block had solidified, it was removed from the Eppendorf cap and placed in a tissue cassette, processed, and embedded in paraffin. A cell line microarray of 3-fold redundancy of the cell lines was constructed in the same method as the tissue microarray described above.

Immunofluorescence staining. The tissue microarray and cell line microarray slides were deparaffinized by two xylene rinses followed by two rinses with 100% ethanol. Antigen retrieval was done by boiling the slides in a pressure cooker in a sodium citrate buffer (pH 6.0). After rinsing briefly in 1× TBS, a 30-minute incubation with 2.5% hydrogen peroxide/methanol was used to block endogenous peroxidases. To reduce nonspecific background staining, slides were incubated with 0.3% bovine serum albumin/1× TBS for 1 hour at room temperature, followed by a series of 2-minute rinses in 1× TBS, 1× TBS/0.01% Triton, and 1× TBS (TBS washes). Slides were incubated overnight at 4°C with a monoclonal

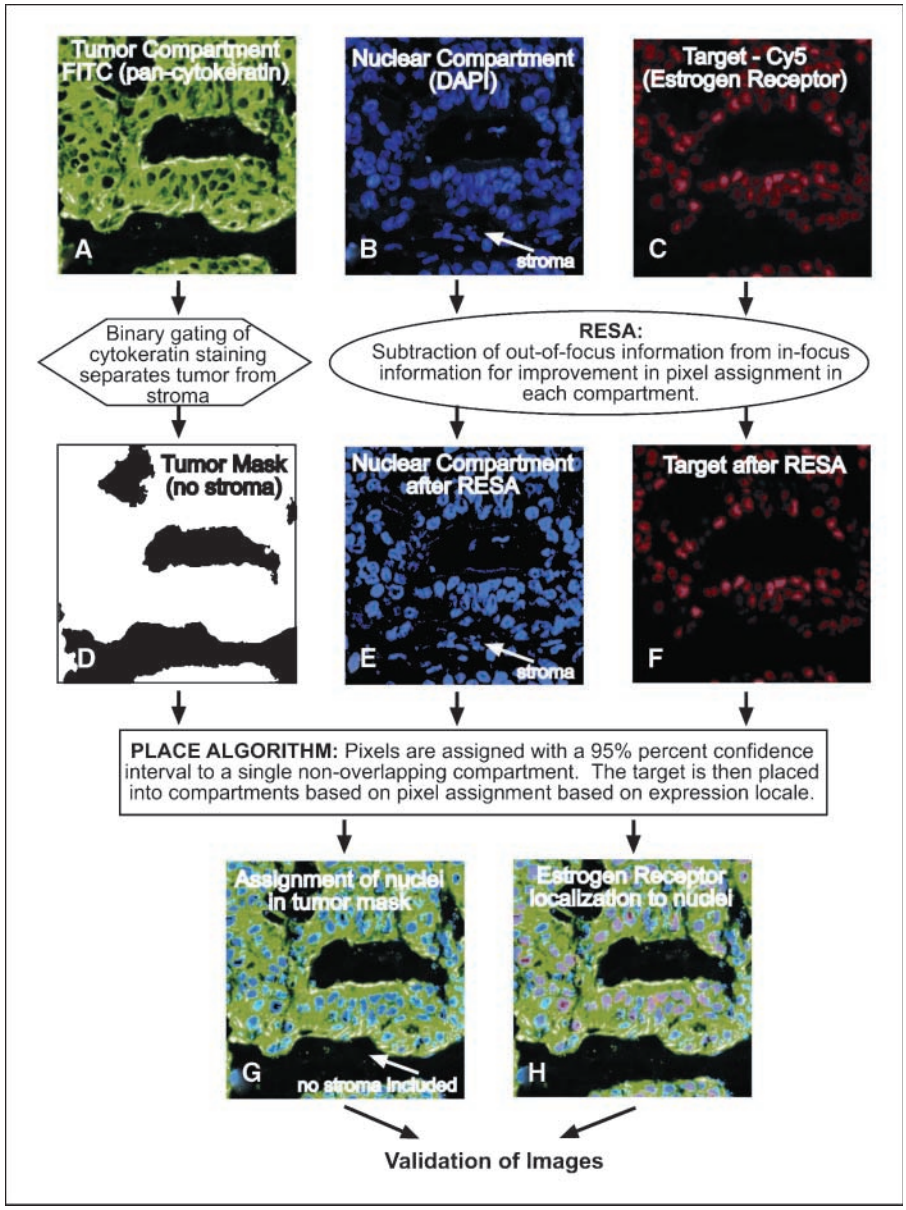

Figure 1. Diagram of AQUA method of analyzing protein expression levels. *A* to *C,* artificially colored images of the cytokeratin staining at the FITC wavelength (*A*), DAPI staining of nuclei (*B*), and ER staining (*C*). In the progression from (*A*) to (*D*), the epithelial tumor is separated from the surrounding stroma by binary gating of the cytokeratin staining to form a tumor ''mask'' that excludes stroma. The DAPI (*B*) and Cy5 (*C*) images are processed through the RESA algorithm, which is the subtraction of out-of-focus information from in-focus information for improvement in pixel assignment in each compartment as shown in (*E* and *F*). Note that the DAPI images contain stromal nuclei, which will later be filtered out by only including those nuclei that fall within the masked tumor region (*G*). The PLACE algorithm is a method to assign pixels with a 95% confidence interval to a single nonoverlapping compartment as shown by the placement of nuclei within the epithelial tumor region only (*G*). The target is then placed into compartments based on its pixel assignment to the defined subcellular compartments, as illustrated by the nuclear localization of ER (*H*).

mouse anticytokeratin antibody (clone AE1/AE3, DAKO, Carpinteria, CA, 1:100) for the HER2 slides and a rabbit anticytokeratin antibody (1:100, DAKO) for the β-catenin, ER, PR, and Ki-67 slides. Slides were hybridized with either HER2 (c-erbB-2 oncoprotein, 1:8,000 dilution for 1 hour, DAKO), β-catenin (clone 14, 1:500 overnight incubation, BD Biosciences, San Jose, CA), ER (clone ID5, 1:50 dilution for 1 hour, DAKO), PR (clone 636, 1:50 dilution for 1 hour, DAKO), or Ki-67 (clone B56, 1:200 overnight incubation, BD Biosciences). Slides were washed in 1× TBS rinses and incubated with secondary antibodies for 1 hour at room temperature as follows: Alexa 488 goat anti-mouse or Alexa 488 goat anti-rabbit (1:100, Molecular Probes, Eugene, OR) for detecting cytokeratin and species-specific horseradish peroxidase (HRP) with a dextran-polymer backbone (Envision, DAKO) along with 4′,6-diamidino-2-phenylindole (DAPI, 1:100, DAKO) for visualization of nuclei. For Ki-67 detection, double amplification was needed. This was accomplished by following the Envision reagent step with incubation with biotin tyramide (1:50 dilution for 10 minutes, Perkin-Elmer, Wellesley, MA) and then HRP-streptavidin (1:200 dilution for 30 minutes, Perkin-Elmer). All slides were washed with TBS rinses followed by a 10-minute incubation with Cy-5 tyramide (1:50 dilution in Amplification Diluent, Perkin-Elmer). The slides were mounted in 0.6% *n*-propyl gallate (an antifade mounting medium) and coverslipped.

AQUA analysis of tissue and cell line microarrays. The AQUA software linked to the fluorescence microscopy system allowed for quantification of the protein of interest within the tumor region of each tissue microarray core (Fig. 1; ref. 12). Briefly, pan-cytokeratin is used to separate epithelial tumor from surrounding stroma, and different fluorescent tags (i.e., DAPI) are used to demarcate subcellular compartments (Fig. 1*A* and *D*). Due to the thickness of the tissue sections and the resulting overlap of subcellular compartments, an exponential subtraction algorithm (RESA) is used to subtract an out-of-focus image from an in-focus image, thereby providing improved pixel assignment to subcellular compartments. At the Cy-5 wavelength, which is outside the range of tissue autofluorescence, the target of interest is tagged and measured within the subcellular compartments by the PLACE algorithm (see Fig. 1). As illustrated by the images of ER staining in the diagram of the AQUA method in Fig. 1, the first step of quantification was the capture of the cytokeratin staining for each breast cancer core (Fig. 1*A*). Nuclear regions were delineated by taking an image of DAPI staining (Fig. 1*B*), which shows stromal nuclei as well as epithelial nuclei and defines a nuclear

compartment. Coalescence of cytokeratin staining at the membrane was used to define the membrane compartment for analysis of HER2 and β-catenin staining. The image of the marker of interest [β-catenin, ER, HER2, Ki-67, or progesterone receptor (PR)] were captured at the Cy-5 wavelength (Fig. 1*C*). In-focus and out-of-focus images were captured at each wavelength. The compartments used for analyses were nuclear and membranous β-catenin staining, nuclear ER staining, nuclear progesterone staining, nuclear Ki-67 staining, and membranous HER2 staining. The resulting AQUA score is the measurement of the biomarker pixel intensity within a compartment divided by the total area of the compartment (to normalize for differences in tumor area in each spot). Tissue microarray cores without sufficient breast tumor epithelium (<5% of total area is under the keratin mask) were excluded from the analysis, which reduced the total number of specimens evaluated for each of the biomarkers to between 452 and 576 samples included in later analyses.

Statistical analysis. Statistical analyses using Cox proportional hazards and Kaplan-Meier survival curves (with their significance analyzed by the Mantel-Cox log-rank test) were completed using Statview 5.0.1 (SAS Institute, Inc., Cary, NC). The cohort was split into a matched training and validation set using a function of the X-tile software (24) as a method for selection of optimal cutpoints.[1] This is achieved by the calculation of a log-rank χ^2 statistic for every possible division of the cohort expression data. It is then divided into either two or three optimal groups that are ordinal indicators of risk based on the continuous input variable. The results are plotted on a two-dimensional graph in which each pixel is colored proportionally to its χ^2 value. The maximum χ^2 value is automatically determined by X-tile and is designated as the cutpoint for optimal parsing of the protein expression data. X-tile also allows for training set/validation set analysis to validate the cutpoint selection. The training set and validation set were randomly assigned to generate two groupings with equivalent baseline survival curves for all patients with values for all three markers and both censor and follow-up information.

Results

To be able to rigorously measure the concentration of β-catenin the tumor samples, total β-catenin protein levels (as ng/mg protein lysate) were detected by ELISA and by AQUA analysis of the same cell lines embedded into a tissue microarray. The cell lines selected showed a range of protein expression levels by ELISA. NCI-H28 cells, which have been shown to have a deletion in the *β-catenin* gene (33), are used as a 0 point and the others are shown ranging to 823.45 ng/mg for SW-480 (Fig. 2). Comparison of the AQUA scores of the embedded cell lines and the ELISA concentrations showed an correlation of 0.853 (Fig. 2). The calculation of these cell line concentrations provided an embedded standard curve for the conversion of β-catenin AQUA scores to a specific concentration for each of the tumor samples. The resultant range of β-catenin concentration of the tumors was between 3.88 and 15,893.64 ng/mg. Examples of immunofluorescence staining for β-catenin are shown in Fig. 3 with a high β-catenin-expressing tumor shown in Fig. 3*A* and a low β-catenin protein–expressing tumor in Fig. 3*B*. We found very few cases (<10) with nuclear staining; thus, for the remainder of the analysis, we assessed only β-catenin staining within the membrane compartment.

To observe the relationship between β-catenin and patient outcome in a manner similar to that used for immunohistochemical data, but also in a rigorous manner for continuous data, we needed to find optimal cutpoints. Historically, this is often done by simply choosing quartile or quintile, but those methods do not optimize for biological variability. Thus, we applied a recently developed statistical method called X-tile (24) to determine the optimal divisions of a continuous population and then do statistical testing using training set/validation set methods. The X-tile plots provide an assessment of every division of the continuous β-catenin AQUA data into low-, middle-, and high-level expression, whereby each point in the triangular grid represents a different cutpoint. The intensity and color of each pixel in the X-tile plot represents the strength and direction of the relationship with patient outcome, respectively. This approach uses the power of the continuous data but then converts the data into ordinal classes for the sake of comparative statistical analysis.

The optimal AQUA low cutpoint as determined from the β-catenin training set was 19.17 ng/mg and the high cutpoint was 109.53 ng/mg (n = 222, Fig. 4*A* and *B*). The green color of the pixels in the X-tile plot shows that patients with high levels of membranous β-catenin have a better prognosis than those with lower levels in a continuous manner at many different possible cutpoints. The low population consists of 58 patients (36.21% censored), the middle population has 124 patients (54.84% censored), and the high population has 40 patients (70.00% censored). Because χ^2 values were used to determine the optimal cutpoint, it is not statistically valid to test this same data for significance by the log-rank test. Instead, the cutpoints must be tested on a unique, nonoverlapping validation set (n = 223; Fig. 4*C* and *D*). Using the cutpoints from the training set, we find 58 patients classified as low (36.21% censored), 125 classified as middle (55.20% censored), and 40 patients classified as high (67.50% censored). This resulted in a Kaplan-Meier log-rank test χ^2 value of 13.764 and a P value of 0.0010, suggesting that a highly statistically significant worse outcome is associated with decreased expression of β-catenin in the membranous compartment. Note that very few cases showed nuclear expression and no associations with outcome were found for this subset.

Univariate and multivariate analyses were completed using the Cox proportional hazards model to assess the predictive value of the biomarkers in this study. The nominalized variables of patient

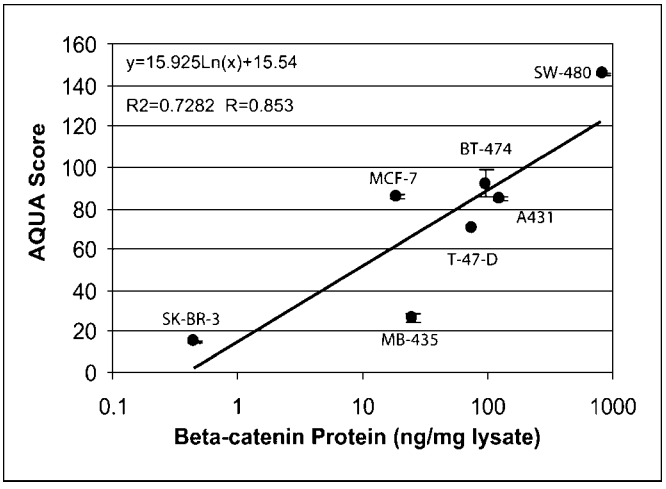

Figure 2. β-catenin ELISA analysis and quantification by AQUA. The concentration of total β-catenin in cell lines (ng/mg total protein in the lysate) was measured by ELISA and is shown for each of the seven cell lines assessed. The concentration is plotted on the *X* axis on a log scale against the AQUA scores. The AQUA scores are the average of a triplicate measurement for each cell line. The regression shows a correlation of 0.853.

[1] X-tile software can be downloaded at http://www.tissuearray.org/rimmlab/.

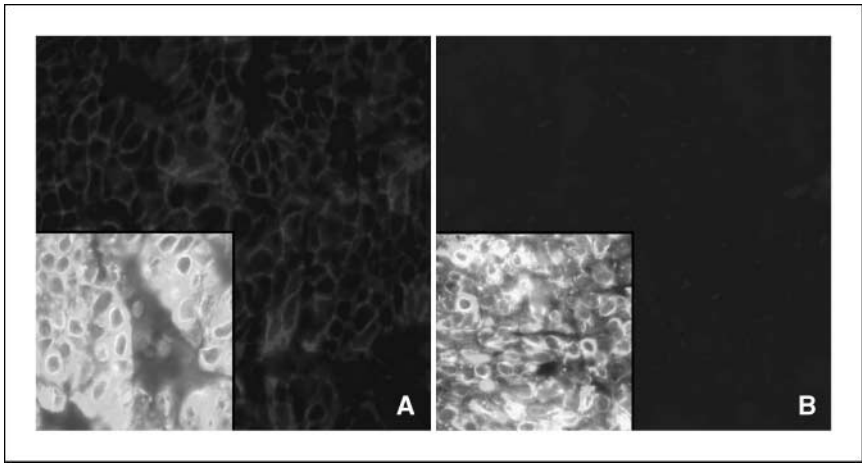

Figure 3. Immunofluorescent staining of breast cancer tissue microarrays. The images shown are ×40 magnification immunofluorescence images of tissue microarray tumor staining. *A,* artificially colored Cy-5 image of high β-catenin expression (*red*); *inset,* cytokeratin (*green*) and DAPI staining (*blue*) in that section of the tumor. *B,* tumor sample with low β-catenin expression; *inset,* cytokeratin and DAPI staining.

age at diagnosis, nodal status, nuclear grade, histologic grade, and tumor size were each assessed by univariate analysis. As shown in Table 1, the univariate analysis of each of the clinicopathologic variables shows that there is a significant relationship between patient survival and nodal status (hazard ratio, 2.4; $P < 0.0001$), nuclear grade (hazard ratio, 1.6; $P = 0.0028$), and tumor size (hazard ratio, 2.6; $P < 0.0001$), but not with patient age or histologic grade. All five of the standard biomarkers that were quantitatively assessed by AQUA show statistical significance by univariate analysis (Table 2) with hazard ratios ranging from 1.4 to 2.6.

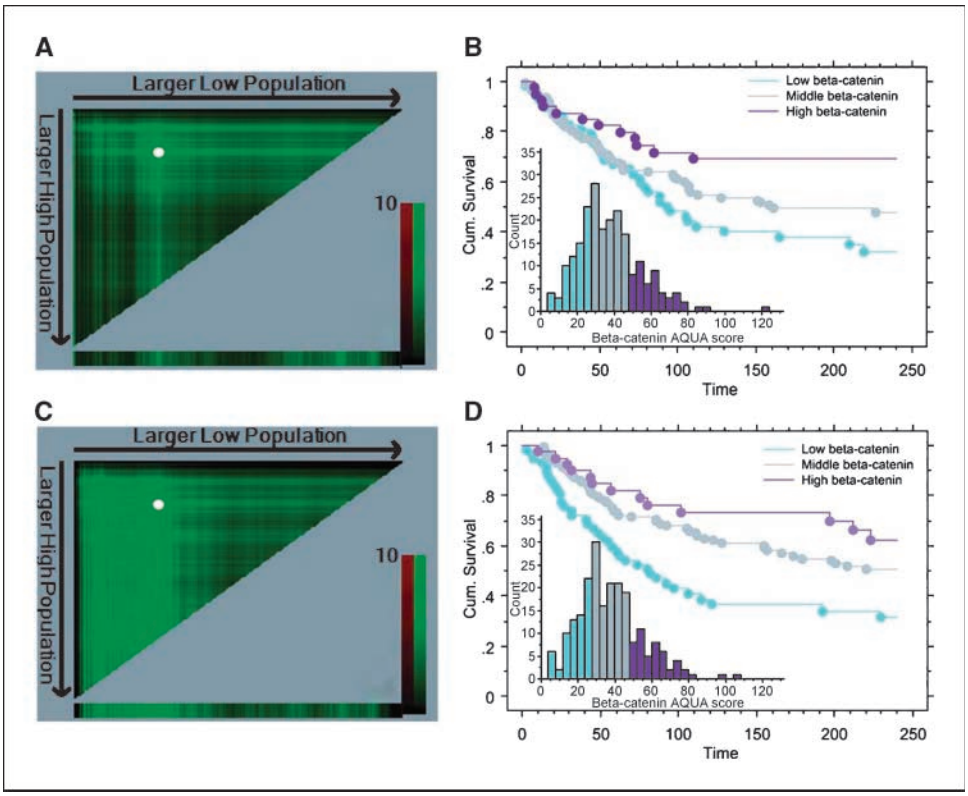

Figure 4. X-tile plots of β-catenin expression optimal cutpoint selection by training set and test set validation. X-tile plots represent all possible divisions of the β-catenin data for the training set (*A*) and test set (*C*) into a low, middle, and high population. Each pixel represents an individual cutpoint where the number of patients in the group increases as you progress down for the high-expression group, or to the right for the low-expression group. Interpretation of these graphs and further examples are seen in our previous article on the topic (24). The intensity is proportional to the χ^2 value and the color of the pixel represents the direction of the relationship with patient survival if assessed by Kaplan Meier analysis (*B* and *D*). *X axis* (*A* and *C*), all of the possible high populations, with the number of patients designated as "high" increasing as the *X* axis increases. *Y axis,* all of the possible low populations, with an increase in the *Y* axis representing an increasing number of patients designated as "low." The hypotenuse of the triangle is the region where all cases are either high or low. The range of cutpoint associations with patient outcome is shown ranging from a weak relationship (*black pixel coloration*) to a strong relationship (*bright green,* inverse relationship; *bright red,* direct relationship) based on the χ^2 value of each individual association. The optimal division (i.e., the highest χ^2 value) was selected as the cutpoint in the training set denoted by the solid circle (*A*), with its Kaplan-Meier curve shown in (*B*). This same cutpoint was selected in the test set denoted by the solid circle (*C*), giving a validation *P* value of 0.0016 and its Kaplan-Meier curve shown in (*D*). *Blue population,* low group; *gray,* middle group; *pink,* high group (in the histograms and the survival curves). *Inset* (*B* and *D*), histograms of the membranous β-catenin AQUA scores (*Y axis*) graphed by number of patients (*X axis*).

Table 1. Cox univariate analysis of breast cancer samples with ordinal clinical variables (20-year survival)

Variable	No. samples*	Hazard ratio (95% confidence interval)	P
Age at diagnosis (y)	604		
≤50	176	1.000	
>50	428	1.207 (0.927-1.572)	0.1629
Histologic grade	297		
1	13	1.000	
2	164	1.354 (0.593-3.094)	0.4715
3	120	1.564 (0.680-3.593)	0.2924
Nodal status	604		
Node negative	310	1.000	
Node positive	294	2.408 (1.886-3.075)	<0.0001
Nuclear grade	553		
1	105	1.000	
2	294	1.004 (0.719-1.402)	0.9812
3	154	1.574 (1.107-2.237)	0.0116
Tumor size (cm)	558		
≤2	270	1.000	
>25	192	1.607 (1.209-2.137)	0.0011
≥5	96	2.617 (1.905-3.594)	<0.0001

*Includes only those samples both with follow-up information and measurements for a particular marker.

For the multivariate analyses, a model was constructed to include all five biomarkers as well as the clinical variables suggested by univariate analysis (patient age, nuclear grade, nodal status, and tumor size). Table 3 shows that age, node status, tumor size, ER, PR, Ki67, and β-catenin are all independently predictive of outcome. The hazard ratio ranges from 1.4 for PR to 6.8 for β-catenin.

Discussion

Using an objective and quantitative approach to assess β-catenin expression, we find that decreased membranous expression is highly associated with poor outcome. The 20-year survival in the low expressing group is 38% compared with 76% in the high expressers. We also find that low expression of this biomarker is highly prognostic of poor outcome by multivariate analysis showing a hazard ratio of 6.8. Thus, we believe it could be useful as a prognostic marker or as part of a prognostic index for prediction of the aggressiveness of breast cancer. A caveat to these results is that they are derived using a method for optimal cutpoint selection, because the use of AQUA-based analysis results in continuous quantitative data. In efforts to diminish the chances of overfitting the data, we have selected outcome-matched training and validation sets as described above. We have also considered other hazards associated with optimal cutpoint selection as described in our previous work (24). However, this work, like all other works on the topic of β-catenin expression in breast cancer, is a retrospective study that requires prospective validation.

The predominant staining pattern for β-catenin this cohort was membranous. This is consistent with most of the other studies in the literature, as well as a previous study of breast cancer tumors from our laboratory by Chung et al. (28). However, the paper from the Hung group is in direct conflict with this result (11). Furthermore, there is abundant evidence from more basic experiments suggesting an important role for *wnt* signaling in breast cancer (reviewed in refs. 4, 5). For example, transgenic *wnt* expression leads to mammary lobular hyperplasia and ultimately carcinoma as reviewed by Smalley and Dale (34, 35).

Furthermore, transgenic mutant β-catenin expressed in mouse mammary glands leads to carcinoma (36). If *wnt* signaling is important, then β-catenin should be present in the nucleus to activate the lymphoid enhancer factor/T-cell factor transcriptional complex. There are a number of possible explanations for this apparent discrepancy. One possibility is that the level of β-catenin in the nucleus is too low to be detected by our assay. However, to our knowledge, no one has measured the level of β-catenin in the nucleus of cells in the *wnt* model systems. Furthermore, in breast cancers from mice expressing mutant β-catenin, immunofluorescent assays did not reveal either mutant or wild-type β-catenin in the nucleus (36). A second possibility is that it is not present in the nucleus, but rather *wnt* signals via some alternative mechanism (noncanonical *wnt* signaling; ref. 37). A third possible explanation is the antibody selection. Because different antibodies have different affinity, it is possible that different studies would show disparate results as a function of antibody selection. We feel this is less likely because this antibody had previously shown nuclear and membranous staining in both colon carcinoma (12) and melanoma samples (38). Furthermore, the antibody used by the Hung group is not published in Lin et al, so it is difficult to compare to other studies. In summary, we believe that the minimal amount of β-catenin found in the nucleus in breast cancer samples is reflective of the biology rather than an antibody detection artifact.

The Chung et al. (28) breast cancer study from our laboratory used only the node-negative cases and showed no relationship between expression and outcome. That study investigated β-catenin expression in conjunction with other components of the *wnt* signaling pathway. There was no marked nuclear staining

Table 2. Cox univariate analysis of breast cancer samples with continuous variables (20-year survival) converted to ordinal categories using X-tile optimal cutpoints

Marker	No. samples*	Hazard ratio (95% confidence interval)	P
β-catenin			
High	82		
Low	117	2.663 (1.689-4.198)	<0.0001
Middle	252	1.702 (1.103-2.626)	0.0162
ER (low)	409 (118, 291)†	1.624 (1.206-2.185)	0.0014
HER2 (high)	518 (454, 54)	1.526 (1.036-2.249)	0.0325
Ki-67 (high)	434 (71, 363)	1.623 (1.077-2.446)	0.0206
PR (low)	412 (198, 214)	1.463 (1.113-1.923)	0.0063

*Includes only those samples both with follow-up information and measurements for a particular marker.
†The parenthesis contain first the number of samples in the "low" group followed by the number of samples in the "high" group (i.e., n = low, n = high).

Table 3. Cox multivariate analysis of breast cancer samples (20-year survival, $n = 257$)

Variable	Hazard ratio (95% confidence interval)	P
Age at diagnosis (>50 y)	1.810 (1.141-2.872)	0.0118
Nodal status (node positive)	1.993 (1.345-2.954)	0.0006
Nuclear grade		
1	1.0	
2	1.064 (0.633-1.789)	0.8152
3	1.404 (0.773-1.789)	0.2653
Tumor size (cm)		
≤2	1.0	
>2-5	1.847 (1.210-2.820)	0.0045
≥5	3.003 (1.865-4.836)	<0.0001
ER (low)	2.786 (1.770-4.385)	<0.0001
PR (low)	1.453 (1.002-2.108)	0.0490
HER2 (high)	1.284 (0.649-2.541)	0.4271
Ki-67 (high)	2.043 (1.153-3.618)	0.0143
β-catenin		
High	1.0	
Middle	4.286 (2.058-8.926)	0.0001
Low	6.808 (3.061-15.140)	<0.0001

NOTE: The results of the training set and validation set were combined for this multivariate analysis and histologic grade was excluded due to the large number of tumors without data for this variable.

in the tumors and there was no prognostic value of membranous staining of β-catenin in this cohort. We feel that this is an example of how quantitative immunofluorescence is a more sensitive and objective measure of protein expression than semiquantitiative subjective brown stain by-eye scoring of samples. We have shown previously that AQUA analysis is able to find associations between protein expression and patient outcome that were not seen when the same samples were evaluated by semiquantitative by-eye analysis (12, 27). When the continuous β-catenin expression data in this study was analyzed on the entire cohort separating patients by nodal status, membranous β-catenin was a stronger predictor of survival in univariate analysis for the 230 node-positive cases ($P = 0.0077$, data not shown) than in the 221 node-negative cases ($P = 0.0158$, data not shown). Therefore, it is not surprising that this relationship was missed by semiquantitative immunohistochemical analysis of β-catenin only in node-negative cases.

This study is the largest quantitative cohort examination of β-catenin protein levels and patient outcome to date. The use of AQUA has allowed us to generate an objective, continuous data set of protein expression levels for biomarkers of interest rather than ordinal semiquantitative scores. Use of β-catenin ELISAs to determine protein concentration in cell lines, followed by AQUA analysis of those same cell lines as cores in tissue microarrays, allowed us to generate a standard curve of β-catenin protein expression. This allowed us to quantitatively determine the β-catenin protein concentration in the tumor tissue microarray cores. Our results show that high levels of membranous β-catenin protein expression predict better prognosis both through univariate analysis and training set/validation set analysis by X-tile. β-Catenin is an independent predictor of patient outcome as shown by multivariate analysis that included standard clinicopathologic variables and standard breast cancer biomarker assessments on a continuous level.

Although there is currently no Food and Drug Administration–approved therapeutic targeting β-catenin (perhaps by stabilizing it on the membrane), studies are under way that are targeting the *wnt* pathway. Furthermore, even in the absence of predictive value, this study suggests prognostic value of assessment of membranous β-catenin expression. We believe that it could be valuable as an independent marker or as a component of a series of markers designed to predict recurrence or outcome in breast cancer.

Acknowledgments

Received 1/10/2006; revised 2/14/2006; accepted 3/9/2006.

Grant support: Patrick and Catherine Weldon Donaghue Foundation for Medical Research, NIH grant NCI R21 CA100825, and U.S. Army grant DAMD-17-02-0463 (D.L. Rimm); U.S. Army Breast Cancer Research grant DAMD17-03-1-0349 (M. Dolled-Filhart); NIH Medical Scientist Training Program (J. Giltnane); NIH grant K0-8 ES11571 (R.L. Camp); and the Breast Cancer Alliance of Greenwich, Connecticut (D.L. Rimm and R.L. Camp).

The costs of publication of this article were defrayed in part by the payment of page charges. This article must therefore be hereby marked *advertisement* in accordance with 18 U.S.C. Section 1734 solely to indicate this fact.

References

1. Hatsell S, Rowlands T, Hiremath M, Cowin P. β-Catenin and Tcfs in mammary development and cancer. J Mammary Gland Biol Neoplasia 2003;8:145–58.
2. Polakis P. Wnt signaling and cancer. Genes Dev 2000; 14:1837–51.
3. Candidus S, Bischoff P, Becker KF, Hofler H. No evidence for mutations in the α- and β-catenin genes in human gastric and breast carcinomas. Cancer Res 1996; 56:49–52.
4. Howe LR, Brown AM. Wnt signaling and breast cancer. Cancer Biol Ther 2004;3:36–41.
5. Brown AM. Wnt signaling in breast cancer: have we come full circle? Breast Cancer Res 2001;3:351–5.
6. Dillon D, Johnson C, Rimm DL, Costa J. K-ras mutational analysis as a routine adjunct in the cytologic diagnosis of pancreatobiliary neoplasms. Lab Invest 1998;78:37a.
7. Nakopoulou L, Gakiopoulou H, Keramopoulos A, et al. c-Met tyrosine kinase receptor expression is associated with abnormal β-catenin expression and favourable prognostic factors in invasive breast carcinoma. Histopathology 2000;36:313–25.
8. Karayiannakis AJ, Nakopoulou L, Gakiopoulou H, et al. Expression patterns of β-catenin in *in situ* and invasive breast cancer. Eur J Surg Oncol 2001;27:31–6.
9. Bukholm IK, Nesland JM, Karesen R, Jacobsen U, Borresen-Dale AL. E-cadherin and α-, β-, and γ-catenin protein expression in relation to metastasis in human breast carcinoma. J Pathol 1998;185:262–6.
10. Bankfalvi A, Terpe HJ, Breukelmann D, et al. Immunophenotypic and prognostic analysis of E-cadherin and β-catenin expression during breast carcinogenesis and tumour progression: a comparative study with CD44. Histopathology 1999;34:25–34.
11. Lin SY, Xia W, Wang JC, et al. β-Catenin, a novel prognostic marker for breast cancer: its roles in cyclin D1 expression and cancer progression. Proc Natl Acad Sci U S A 2000;97:4262–6.
12. Camp RL, Chung GG, Rimm DL. Automated subcellular localization and quantification of protein expression in tissue microarrays. Nat Med 2002;8: 1323–7.
13. Bondi J, Bukholm G, Nesland JM, Bukholm IR. Expression of non-membranous β-catenin and γ-catenin, c-Myc and cyclin D1 in relation to patient outcome in human colon adenocarcinomas. APMIS 2004;112:49–56.
14. Ryo A, Nakamura M, Wulf G, Liou YC, Lu KP. Pin1 regulates turnover and subcellular localization of β-catenin by inhibiting its interaction with APC. Nat Cell Biol 2001;3:793–801.
15. Pedersen KB, Nesland JM, Fodstad O, Maelandsmo GM. Expression of S100A4, E-cadherin, α- and β-catenin in breast cancer biopsies. Br J Cancer 2002;87:1281–6.
16. Wong SC, Lo SF, Lee KC, et al. Expression of frizzled-related protein and Wnt-signalling molecules in invasive human breast tumours. J Pathol 2002;196:145–53.
17. Gillett CE, Miles DW, Ryder K, et al. Retention of the expression of E-cadherin and catenins is associated with shorter survival in grade III ductal carcinoma of the breast. J Pathol 2001;193:433–41.
18. Battifora H. The multitumor (sausage) tissue block: novel method for immunohistochemical antibody testing. Lab Invest 1986;55:244–8.

19. Wan WH, Fortuna MB, Furmanski P. A rapid and efficient method for testing immunohistochemical reactivity of monoclonal antibodies against multiple tissue samples simultaneously. J Immunol Methods 1987;103:121–9.

20. Kononen J, Bubendorf L, Kallioniemi A, et al. Tissue microarrays for high-throughput molecular profiling of tumor specimens. Nat Med 1998;4:844–7.

21. Camp RL, Charette LA, Rimm DL. Validation of tissue microarray technology in breast carcinoma. Lab Invest 2000;80:1943–9.

22. Zhang D, Salto-Tellez M, Putti TC, Do E, Koay ES. Reliability of tissue microarrays in detecting protein expression and gene amplification in breast cancer. Mod Pathol 2003;16:79–84.

23. Torhorst J, Bucher C, Kononen J, et al. Tissue microarrays for rapid linking of molecular changes to clinical endpoints. Am J Pathol 2001;159:2249–56.

24. Camp RL, Dolled-Filhart M, Rimm DL. X-tile: a new bio-informatics tool for biomarker assessment and outcome-based cut-point optimization. Clin Cancer Res 2004;10:7252–9.

25. Dolled-Filhart M, Rimm DL. Tissue arrays. 7th ed. In: DeVita VT, Jr., Hellman S, Rosenberg SA, editors. Cancer: principles and practice of oncology. Philadelphia: Lippincott Williams and Wilkins; 2004. p. 26–34.

26. Dolled-Filhart MP, Rimm DL. Tissue microarray technology: a new standard for molecular evaluation of tissue? Princ Pract Oncol Technol Update 2002;16: 1–11.

27. Camp RL, Dolled-Filhart M, King BL, Rimm DL. Quantitative analysis of breast cancer tissue microarrays shows that both high and normal levels of HER2 expression are associated with poor outcome. Cancer Res 2003;63:1445–8.

28. Chung GG, Zerkowski MP, Ocal IT, et al. β-Catenin and p53 analyses of a breast carcinoma tissue microarray. Cancer 2004;100:2084–92.

29. Dolled-Filhart M, Camp RL, Kowalski DP, Smith BL, Rimm DL. Tissue microarray analysis of signal transducers and activators of transcription 3 (Stat3) and phospho-Stat3 (Tyr705) in node-negative breast cancer shows nuclear localization is associated with a better prognosis. Clin Cancer Res 2003;9:594–600.

30. Kang JY, Dolled-Filhart M, Ocal IT, et al. Tissue microarray analysis of hepatocyte growth factor/Met pathway components reveals a role for Met, matriptase, and hepatocyte growth factor activator inhibitor 1 in the progression of node-negative breast cancer. Cancer Res 2003;63:1101–5.

31. Kluger HM, Dolled-Filhart M, Rodov S, et al. Macrophage colony-stimulating factor-1 receptor expression is associated with poor outcome in breast cancer by large cohort tissue microarray analysis. Clin Cancer Res 2004;10:173–7.

32. Tolgay Ocal I, Dolled-Filhart M, D'Aquila TG, Camp RL, Rimm DL. Tissue microarray-based studies of patients with lymph node negative breast carcinoma show that met expression is associated with worse outcome but is not correlated with epidermal growth factor family receptors. Cancer 2003;97:1841–8.

33. Shigemitsu K, Sekido Y, Usami N, et al. Genetic alteration of the *β-catenin* gene (CTNNB1) in human lung cancer and malignant mesothelioma and identification of a new 3p21.3 homozygous deletion. Oncogene 2001;20:4249–57.

34. Smalley MJ, Dale TC. Wnt signalling in mammalian development and cancer. Cancer Metastasis Rev 1999; 18:215–30.

35. Smalley MJ, Dale TC. Wnt signaling and mammary tumorigenesis. J Mammary Gland Biol Neoplasia 2001;6: 37–52.

36. Imbert A, Eelkema R, Jordan S, Feiner H, Cowin P. ΔN89 β-catenin induces precocious development, differentiation, and neoplasia in mammary gland. J Cell Biol 2001;153:555–68.

37. Gonzalez-Sancho JM, Brennan KR, Castelo-Soccio LA, Brown AM. Wnt proteins induce dishevelled phosphorylation via an LRP5/6-independent mechanism, irrespective of their ability to stabilize β-catenin. Mol Cell Biol 2004;24:4757–68.

38. Kielhorn E, Provost E, Olsen D, et al. Tissue microarray-based analysis shows phospho-β-catenin expression in malignant melanoma is associated with poor outcome. Int J Cancer 2003;103:652–6.